Quantum Gyroscope with Nitrogen-Vacancy Centers: A Theoretical and Applied Review

Vikram Gangu[1]

Received April 28, 2026
Accepted July 26, 2026
Electronic access August 15, 2026

Diamond nitrogen vacancy (NV) center gyroscopes benefit from a carbon-lattice with a low nuclear spin background which stabilizes their electron and nuclear spins enabling long coherence times. Unlike gas-based nuclear magnetic resonance (NMR) gyroscopes and spin-exchange relaxation free (SERF) atomic spin gyroscopes, the crystal lattice nature of diamond allows NV center point defects embedded in them to function as quantum sensors even at room temperature and pressure. These unique qualities combined with scalability and potential for miniaturization, make them crucial for both civilian and military applications, especially in Global Positioning System (GPS)-denied environments and underwater explorations. Of the various performance metrics of quantum gyroscopes, sensitivity emerges as the key parameter for most applications. NV center gyroscopes are expected to reach sensitivity performance of gas-phase NMR and SERF atomic gyroscopes at a scalability comparable to micro-electromechanical systems (MEMS). This review synthesizes the technological breakthroughs, error compensation and mitigation measures driving improvements in sensitivity of NV center gyroscopes. The synthesis highlights the trajectory and persistent challenges of the field, addressing a gap in qualitative review literature. An approximately 3.5-order-of-magnitude improvement in sensitivity, from experimentally demonstrated $4.7^\circ/\mathrm{s}/\sqrt{\mathrm{Hz}}$ (physical rotation, optical readout, reported as $4.7^\circ/\sqrt{\mathrm{s}}$) to a model-predicted $1.5\ \mathrm{m}^\circ/\mathrm{s}/\sqrt{\mathrm{Hz}}$ (emulated rotation, cavity readout) has emerged from the cumulative efforts of researchers working on NV center gyroscopes. Connections are made between classical and quantum physics concepts and landmark research findings in the study of NV center gyroscopes to aid emerging researchers.

Keywords: NV center gyroscope, Quantum physics review paper, NMR gyroscope, sensitivity

Introduction

Gyroscopes are devices used for measuring angular velocity used in both consumer and defense applications. Inertial sensors, primarily accelerometers and gyroscopes, provide an internal frame of reference for measurements, in lieu of relying on an external frame of reference. In the recent decades, with miniaturization of instrumentation, like micro-electromechanical system (MEMS), driven by emerging applications, inertial sensors advanced to technologies with no moving parts. Instead they use physical phenomena such as vibrations, light interference, magnetic resonance, atomic interference using cold-atom technology and solid state quantum sensing for measuring parameters of interest[1,2]. In spite of demonstrated high levels of precision for short periods of time, vapor nuclear magnetic resonance (NMR)[3,4] gyroscopes are fragile to magnetic fields. While spin-exchange pumped, spin exchange relaxation free (SERF)[4,5] atomic gyroscopes still require vacuum chamber to minimize unwanted frequency shifts from quantum interactions, this in addition to the high temperature environments required for functioning.

The next section briefly explores various instrumentation errors that affect gyroscope performance. While all these parameters are consequential to practical use of these sensors, this review focuses on sensitivity (closely related to angle random walk) as the primary figure of merit, for two reasons. First, sensitivity is the parameter most actively targeted by current NV center gyroscope research, where improvements are achieved through advances in fundamental physics such as extended coherence times, improved bulk polarization, and enhanced readout fidelity, which are explored further in detail in this review. Second, sensitivity is the parameter where NV center gyroscope research has made the most rapid recent progress illustrated by the demonstrated-to-predicted improvement trajectory.

While this review focuses on sensitivity, the broader case for continued NV center gyroscope research extends to additional parameters not tracked in detail here such as bias drift, long-term stability, multi-functional sensing and environmental resilience. These are discussed briefly in the Conclusion but are not the principal subject of this review. The spin exchange pumped NMR gyroscopes by Northrop Grumman achieved an ARW of $0.005^\circ/\sqrt{\mathrm{h}}$[4] ($\approx 0.08\ \mathrm{m}^\circ/\mathrm{s}/\sqrt{\mathrm{Hz}}$)

[1] *Bergen County Academies, New Jersey, USA*

at a size of 10 cm^3, while research grade SERF-enhanced K-^{3}He atomic gyroscopes have achieved a sensing volume of 0.5 cm^3 for a sensitivity of 5×10^{-7} rad/s/$\sqrt{\text{Hz}}$[5] ($\approx$ 0.029 m°/s/$\sqrt{\text{Hz}}$). Jarmola et al. demonstrated a sensitivity of 4.7°/s/$\sqrt{\text{Hz}}$[6] in a table-top rotation platform of approximately 35 cm diameter, with a reported size of components in μm and mm scale which have the potential to be scaled closer to the size of MEMS gyroscopes. MEMS gyroscopes were classified for an ARW in the range of $0.05 - 0.02°/\sqrt{\text{h}}$ ($\approx 0.8 - 0.3$ m°/s/$\sqrt{\text{Hz}}$) for tactical grade sensors and approaching $< 0.002°/\sqrt{\text{h}}$ (≈ 0.03 m°/s/$\sqrt{\text{Hz}}$) for emerging navigation grade sensors[1]. At an achievable ARW of 1.5 m°/s/$\sqrt{\text{Hz}}$[7], NV center gyroscope research targets approaching NMR sensitivity range at MEMS range size. MEMS is considered a mature technology with multiple decades of engineering improvements reflected in current commercial performance[1,8] while NV center gyroscope technology is in nascent prototype stages[6,9] with multiple physics based pathways for sensitivity improvements[6,7,10] that take advantage of the solid state medium as outlined in the comparative summary tables in this review.

Instrumentation errors

A challenge with inertial sensor errors has been the need for supplemental sensors, and other compensation measures, to correct for errors thus limiting their operational time without external feedback from Global Positioning System (GPS). These errors are categorized as following[11]: Angle random walk (ARW), a noise induced angular error that accumulates with time and closely related to sensitivity (δ_f), defined as the noise floor for detecting a rate signal per unit measurement bandwidth, Bias drift - reporting small rotation when there is none, Thermal noise - mechanical thermal vibrations created due to heat from electronic components, temperature induced frequency shifts, thermal electronic noise, Long-term instability - stemming from cumulative drifts affected by environmental factors that are harder to predict, requiring frequent recalibration or GPS assistance for accurate performance over time and Calibration errors arising from errors in scale factors, alignments etc.

Sensitivity, the minimum reading that can be reliably measured given the noise elements within the device, is tracked as the primary parameter in this review to quantify and explore the accuracy improvements targeted by researchers exploring NV center gyroscopes. ARW and Sensitivity (δ_f) are related mathematically by unit conversion. The scaling factor comes from converting Hrs to secs and Hz to /s: $1°/\sqrt{\text{h}} = 1°/\sqrt{(3600\text{ s})} = 1°/60/\sqrt{\text{s}} \approx 0.01667°/\sqrt{\text{s}} =$ 16.67 m°/s/$\sqrt{\text{Hz}}$, so a gyroscope with $1°/\sqrt{\text{h}}$ ARW has approximately 16.67 m°/s/$\sqrt{\text{Hz}}$ sensitivity. While ARW measures accumulated error, sensitivity measures rate detection floor per square root of bandwidth[6,8,12]. Calibration errors scale with motion and do not accumulate over time, hence these are easier to compensate periodically, while long term stability requires magnetic shielding type mitigation. Solid state sensors, such as diamond nitrogen vacancy (NV) center gyroscopes, are relatively less prone to mechanical thermal noise. Temperature compensated magnets, magnetic shielding etc., are utilized to minimize bias drift and some of the thermal noise components[6,11]. Further correction can be applied using co-magnetometry, including concurrent magnetic field measurement with a second, co-located spin species used to subtract magnetically induced error etc., (see Discussion) to compensate for bias and errors during postprocessing.

Introduction to NV center gyroscopes

In 2012 Ledbetter et al.[13] theoretically proposed the use of diamond NV center gyroscopes as a tool for measuring rotation using quantum spins, the quantum control of a single NV center electron spin in a physically rotating diamond was experimentally demonstrated by Wood et al.[14] in 2018. Following this, Soshenko et al.[9] demonstrated a proof-of-concept nuclear spin gyroscope in 2021. Breakthrough experiments by Jarmola et al., the same year, demonstrated the first NV center gyroscope prototype with measured sensitivity, paving the way for further research. NV Center gyroscopes are analogs of NMR gyroscopes, which are also based on the nuclear spin measurements for sensing but replace less stable gas cells with stable diamond crystal lattice[6]. This facilitates a stable frequency separation for measuring rotation-induced shifts making these functional at standard atmospheric conditions. These gyroscopes are projected to offer long-term stability, low drift, and resilience to environmental noise, compared to MEMS gyroscopes at ambient conditions[2,13] making them highly promising for navigation applications like GPS-denied environments, like underwater, subterranean etc., or long-duration autonomous systems.

This paper answers the question of how the critical parameter of sensitivity has rapidly improved, the scientific advancements that led to their improvement and the persistent challenges to achieving the ‘target’ sensitivity comparable to NMR gyroscopes. While existing reviews address NV center sensing broadly[12,15] or general quantum sensing for navigation[1,2], none focuses on how the NV center gyroscopes sensitivity has advanced since first 2021 demonstrations, addressing various pathways being explored to improve their performance. It also provides a brief background on physical phenomena that govern the functioning of NV center gyroscope. This includes features from both quantum and classical mechanisms including spin states, zero-field splitting, hyperfine and quadrupole interactions, spin readout, bulk polarization, interference, coherence and resonance.

The goal of NV center gyroscope researchers can be consolidated as achieving navigation grade accuracy at costs and size of MEMS sensors for broader applications and scalability[9]. Figure 1 compares the main classes of gyroscopes, viz., mechanical, optical including Fiber-Optic (FOG) and ring laser (RLG), and MEMS, against the improving sensitivity of the NV center gyroscope, the standard quantum limit (SQL) for a given experimental configuration.

Methods

Search methods and selection criteria

A qualitative literature review of published literature in the field of NV center gyroscopes was used to synthesize recent advances and error minimization pathways being pursued by current researchers. The review focused on papers published between 2012 and 2026, drawing primarily from the more recent works from 2021 onwards. Search was conducted using public research databases including arXiv.org, Google Scholar and Lens.org. Search criteria included a combination of keywords: "NV center gyroscope" and "quantum sensor", 'quantum sensing" in the title and/or abstract. To understand the advances made in adjacent but relevant field, 'crystal growth', 'photon collection efficiency', 'multiparameter' and 'multifunctional sensor' were searched with the condition to include NV center in the 'text' category.

The initial Lens.org search for 'NV center' returned approximately 4,700 scholarly works including journal articles, preprints, dissertation, journal issues, reports and books published between 2012 and 2026. Restricting the search to 'NV center gyroscope' in abstract, resulted in only 31 scholarly works, initial screening for duplicates reduced these to 27. Of these, 20 were published 2021 onwards, highlighting the increased momentum in the research of NV center gyroscopes. The abstracts for the 27 articles, published between 2012 and 2026, were reviewed to understand the scope of each paper. Ledbetter et al. provided a general theoretical framework for functioning of an NV center gyroscope and provided historical context, while Jarmola et al. and Soshenko et al., presented complete NV center gyroscope systems integrating multiple subsystem alterations for overall sensitivity improvements and were selected as core papers for the synthesis. Except for G. Wang et al., the remaining 23 abstracts were excluded after abstract review or full text review, for scope mismatch with the review now focusing on sensitivity improvements. References from the two core papers were sought, based on the citation title, context of citation followed by reviewing the abstract where there was potential for scope match. Of the 79 combined references from Jarmola et al. and Soshenko et al., 6 references focusing on general NV physics, NMR gyroscope, and inertial navigation along with 2 additional references, for comparative or supportive points, were chosen. Papers focused on non-Nitrogen isotopes and those with findings superseded by the core papers were excluded.

Ten additional references were identified using topic-based searches, focusing on papers published post 2021 addressing "photon collection efficiency", "coherence time improvement", "cavity enhanced readout", "multi parameter sensing" and from reviewing the abstracts of more recent publications by the previously identified 12 citations. Upon full paper review, H. Wang et al. was found to also present a complete NV center system focused on sensitivity improvements although it was a model based emulated rotation model and hence chosen as the third core paper for the synthesis. Three references were added to address specific gaps in background physics for NV electronic structure, standard quantum limit, quadrupole interaction, that were not adequately covered by the selected references. Six additional references from adjacent fields, specifically gyroscope benchmarking, inertial navigation, sensitivity formulas, were added during manuscript development to support comparative claims. A total of 31 papers were selected to be included as references for this paper.

References for this review were accessed via arXiv.org, sciencedirect.com, APS Journals, except for books and open educational resources accessed through library or their host sites. During manuscript revision, some of the original citations were swapped out preferring peer reviewed sources, and citations updated for the preprints that were published during that time. The two preprints used were flagged at each citation addition to the References section.

Synthesis method

Following a review of the papers, seven were selected for the literature synthesis, with three categorized as core and four as explorative. The core papers were selected for presenting complete NV center gyroscope systems, experimental prototype or emulated model but an end-to-end design that integrates multiple subsystem improvements toward overall sensitivity enhancement. Exploratory papers were selected for focusing on specific subsystem improvements of NV center sensing such as photon collection efficiency, coherence time protection, multi-parameter sensing, or material engineering, which contribute to better functioning of NV center gyroscopes.

Background

In NV center gyroscopes, three phases are involved in sensing angular velocity: initialization, precession and processing:

Initialization: To prepare the sensor for rotation measurement, it is necessary to establish a known quantum state

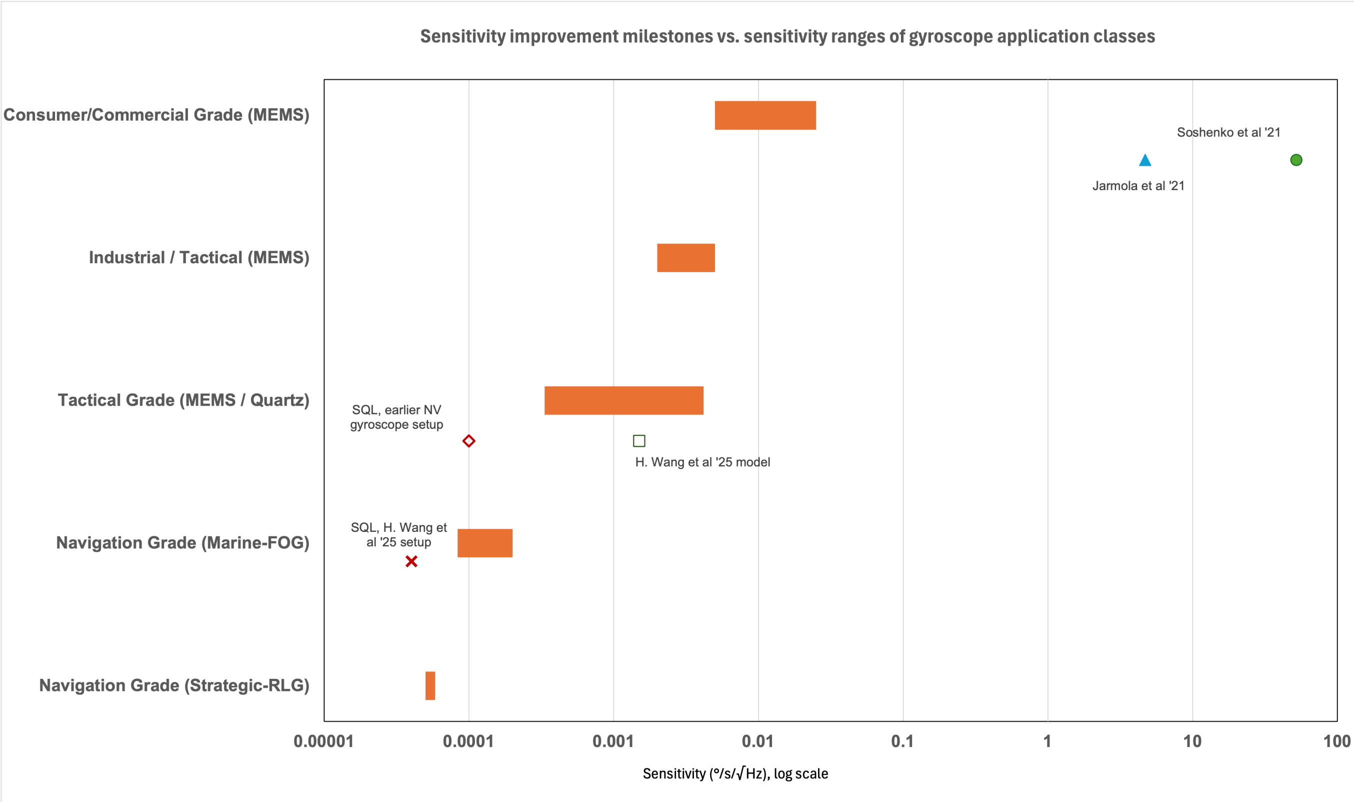

Figure. 1 Demonstrated and predicted NV center gyroscope sensitivities compared against the sensitivity ranges of different gyroscope commercial application classes. The horizontal axis is rotation-rate noise density in $^\circ/\mathrm{s}/\sqrt{\mathrm{Hz}}$ on a logarithmic scale, lower numerical value being desirable. Orange bars show the range of manufacturer-specified rate noise density for each application class, compiled from current vendor datasheets following the survey of Passaro et al.[8] Markers show NV center results by year: Soshenko et al. ($52^\circ/\mathrm{s}/\sqrt{\mathrm{Hz}}$, 2021, green circle) and Jarmola et al.($4.7^\circ/\mathrm{s}/\sqrt{\mathrm{Hz}}$, 2021, blue triangle) are experimental demonstrations while the open square for H. Wang et al. ($1.5\ \mathrm{m}^\circ/\mathrm{s}/\sqrt{\mathrm{Hz}}$, 2025) is a model prediction. The open diamond and 'x' mark the standard quantum limit (SQL) evaluated for previous idealized proposals prior to 2021 and H. Wang et al. configurations, respectively[6,7,9]. The vertical placement of NV markers is for label readability only and does not indicate class membership of cited works. Read chronologically, the markers show sensitivity improvements from the 2021 experimental demonstrations to the 2025 model prediction with the projected SQL approaching navigation-grade performance.

through initialization. This is done through using specific resonant optical pumping laser combined with a radiofrequency or microwave pulses to precisely orient the spins of the NV center. The goal here is to get maximum number of electrons, and hence the nuclei, into a specific quantum spin state i.e., polarization, in order to increase the accuracy of measurement by having more data points.

Precession: After initialization, to sense rotation the NV center must be allowed to precess for an interval. The rotation of the gyroscope then affects electron spins, which are interrelated with nuclear spins, together creating a stable change in the NV center's spin states. The NV center physical rotation is either applied directly or encoded through signal pulse phase changes into the precession changes of the quantum spins. The structure of the NV center ensures that the encoded spin information remains stable enough to be captured during processing.

Processing: The final aspect of the gyroscope's measurement cycle involves measuring some parameter of the NV center that can be used to read its spin change information in order to measure actual rotation. Currently research on NV centers typically measures changes in nuclear spin state between a known initial state and after rotation occurs, using either optical readout[6] or resonant cavity readout systems[7]. High intensity lasers pulse photons at standardized pulse sequence for optical readout NV center gyroscopes and use sequence of microwave pulses for interferometry to use the resultant readout to determine the interval between split spin states. The changes in fluorescence readout, by comparing difference in initial frequency and received frequency, measure the rotational movement in NV center gyroscopes using optical readout[6]. While cavity enhanced microwave mechanisms adopt either dispersive readout or an electromagnetically induced transparent (EIT) readout. Dispersive readout utilizes a detuned probe to induce cavity frequency/phase shifts that are read out for rotation measurement. EIT readout uses two field interference that creates cavity transparency resonant at the nuclear spin transitions. Rotation introduces a shift in this resonance such that the linewidth of the readout is resolvable due to the narrower nuclear spin transition versus electron spin transitions[7,16]. The former is more scalable and cost effective, can be miniaturized further and while the latter provides higher readout fidelity, hence higher sensitivity to rotation measurements.

Spins, spin states, quantum energy states

Electrons possess angular momentum and precession, so they can be visualized as a collection of spinning charges which generate a magnetic dipole. When these electrons pass through a uniform magnetic field, they undergo Larmor precession. This can be visualized as a "wobble" determined by the field strength and the particle's gyromagnetic ratio[15]. Such quantum spin can exist in two distinct states with two values (eigenvalues of $S_z/\hbar$): $+\frac{1}{2}$ or $-\frac{1}{2}$, referred to as spin up or spin down, which correspond to specific energy levels.

The NV^- electronic structure consists of a triplet ground state ($^3A_2$), a triplet excited state (^3E), and intermediate singlet states ($^1A_1$ and ^1E). The $^3A_2$ ground state is split by ~ 2.87 GHz zero-field splitting, into $m_s = 0$ and $m_s = \pm 1$ magnetic sublevels, due to dipolar spin-spin interactions between the two unpaired electrons. Each m_s sublevel is further split by hyperfine coupling due to the ^{14}N nuclear spin and Zeeman interaction with applied magnetic fields. Optical excitation by ~ 532 nm green light drives a transition from $^3A_2$ to ^3E. From ^3E, two competing decay pathways are available, a direct radiative decay back to $^3A_2$ producing red fluorescence and a non-radiative intersystem crossing (ISC) through the singlet manifold mediated by spin-orbit coupling. This branching is spin-selective with $m_s = 0$ sublevels preferring ^3E and $m_s = \pm 1$ preferentially undergoing ISC. However, the non-radiative decay from the singlet states back to $^3A_2$ ground state populates both $m_s = 0$ and $m_s = \pm 1$ sublevels. Over a few optical pumping cycles, this asymmetry of spin dependent and spin independent shifting to and from energy states produces net polarization of the ground state spin into $m_s = 0$, this is the mechanism that enables optical spin initialization in NV center gyroscope operation[15]. Although a nucleus acts as a magnetic dipole similar to an electron it has a much weaker magnetic moment because of its smaller gyromagnetic ratio. This weaker interaction with the environment results in significantly longer coherence times and reduced sensitivity to magnetic noise compared to electron spins. Additionally, these energy states can be manipulated through microwave radiation and radiofrequency for sensing[15].

DQ Ramsey magnetometry protocol

Papers reviewed for this synthesis utilize Double Quantum (DQ)-Ramsey measurement protocols, since compared to Single Quantum (SQ) protocols, the protocol doubles the signal and cancels noise. An initial green laser (~ 532 nm) pulse polarizes the NV ensemble electron spins. This is followed by a sequence of pulses (P_1, P_2) utilizing RF for nuclear spin control and MW pulses for electron manipulation during Ramsey sequence. The signals are read out and manipulated to cancel noise and enhance signal for rotation detection. Refer to Figure 2 for a sample schematic.

Precession time is allowed (τ) to accumulate phase shift due to frequency change and rotation signal. Accumulated phase $\Delta\phi = f_{\mathrm{DQ}}.\tau$ where f_{DQ} is the experimentally measured DQ frequency, and phase shift due to rotation is $\delta f_{\mathrm{DQ}} = \Omega/\pi$ for a rotation signal of Ω. For δf_{DQ} to produce maximum signal and thus increased sensitivity, the working point where the slope of the Ramsey signal is maximum determines the accumulation time. For processing, P_1, P_2 signals are repeated to now, with phase cycling, map the signal again with the accumulated phase shift. Ramsey phase cycling is applied to the signals such that, $R = R_1 - R_2 + R_3 - R_4$, where R_1, R_2, R_3 and R_4 are a combination of P_1, P_2 with phase cycling: $R_1 = \mathrm{P}_1(+\phi) \to \mathrm{P}_2(+\phi), R_2 = \mathrm{P}_1(-\phi) \to \mathrm{P}_2(+\phi), R_3 = \mathrm{P}_1(-\phi) \to \mathrm{P}_2(-\phi), R_4 = \mathrm{P}_1(+\phi) \to \mathrm{P}_2(-\phi)$, with ϕ being the phase of the pulse generator and P_1, P_2 being the first and second rotation pulse. Thus, the phase cycling isolates the rotation induced phase shift while canceling noise induced drifts in phase.

Based on the supplemental information provided in Jarmola et al.[6], sensitivity is then calculated as $\delta_f = \pm\left(\frac{1}{\pi}\cdot\frac{1}{\tau e^{\left(-\tau/T_2^*\right)}}\cdot\frac{\delta V}{V_0 C}\right) = \pm\left(\frac{1}{\pi}\cdot\frac{1}{\tau e^{\left(-\tau/T_2^*\right)}}\cdot\frac{\delta V}{V_H - V_L}\right)$,
where V_H, V_L are the voltage readout or a proportional signal readout for the high and low quantum energy states, V_0 is the brightness (normalization) of voltage fluctuations and C is the contrast evaluated by $V_0 = \frac{V_H + V_L}{2}$ and $C = \frac{V_H - V_L}{V_0}$.

Coherence time, T_2^*, is determined by curve fitting the Ramsey decay and determines maximum feasible precession time τ. N is number of data points such that $N = N_{\mathrm{spins}}.N_{\mathrm{measurements}}$, where N_{spins} are number of NV centers in the diamond ensemble contributing to the measurements and $N_{\mathrm{measurements}}$ are the number of repetitions of the DQ Ramsey sequence. In the long coherence time limit, sensitivity improves approximately as $\sqrt{N}$ and $\sqrt{T_2^*}$ based on the following equation, $\eta \propto \frac{1}{\gamma C\sqrt{N\cdot T_2^*}}$[12], smaller numerical value being better. The more data points there are, the longer the coherence

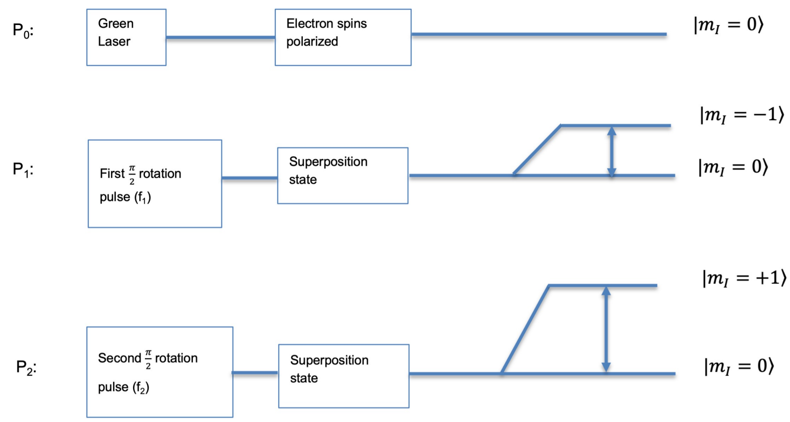

Figure. 2 Schematic of the double-quantum (DQ) Ramsey initialization and measurement protocol. The green laser block is the optical polarization pulse (P_0) that initializes the NV electron spins into a polarized state. The first rotation pulse (P_1), applied at frequency f_1, creates a coherent superposition state that accumulates phase during the free-precession interval; the second rotation pulse (P_2), applied at frequency f_2, projects this accumulated phase back onto a measurable spin-state population. Arrows indicate the sequence of operations, and the superposition states denote the coherent spin states whose accumulated phase encodes the rotation signal.

time and higher readout contrast help improve the sensitivity of an NV center gyroscope setup, but γ, the nuclear gyromagnetic ratio of the sensing nucleus, that is determined by the isotopic material properties, needs to be lower. This is because rotation acts as an effective magnetic field and a smaller γ amplifies the rotation induced signal vs noise. Also, C can range from 0-1 while N and T_2^* can range in multiple orders of magnitude, making them practically more impactful in affecting the sensitivity value.

Standard Quantum Limit (SQL)

The standard quantum limit (SQL) for measuring any single parameter in an NV center is the sensitivity ceiling for measurements using 'N' independent (unentangled) spins. The changes in variable being measured for are mapped as a population difference resulting in a 'stochastic' signal. Even for ideal measurements, the existence of a projection noise of this signal is the basis for SQL. SQL thus defines a minimum detectable signal for detecting angular shifts in a single measurement for an NV center gyroscope and this is proportional to $1/\sqrt{N}$[12]. However, this scaling can be improved if N quantum probes are entangled and act as single quantum system, enhancing the scaling to $1/N$, this is called the Heisenberg limit, which is an absolute quantum-mechanical sensitivity ceiling[17].

The SQL value for a given NV center gyroscope setup, for both experimental and emulated models, is also determined using the parameters that are part of the sensitivity equation discussed in the previous section such as: ensemble size N, coherence time T_2^* and readout contrast C, photon collection efficiency and integration time. While the setups of earlier NV gyroscope proposals had an SQL near 0.1 $\text{m}^\circ/\text{s}/\sqrt{\text{Hz}}$, the larger NV ensemble modeled by H. Wang et al.[7] yields an SQL near 0.04 $\text{m}^\circ/\text{s}/\sqrt{\text{Hz}}$, this is a consequence of the $1/\sqrt{(N \cdot T_2^*)}$ scaling and not a result of change in the readout scheme. The cavity-enhanced readout instead aids in closing the gap between sensitivity achieved and the SQL[7]. To approach SQL optimizing the parameters involved in the sensitivity equation is required while to approach Heisenberg limit, it additionally requires maintaining entangled NV ensembles. Scaling of such approaches has not been pursued in this literature review, however the gap between achievable H. Wang sensitivity value of 1.5 $\text{m}^\circ/\text{s}/\sqrt{\text{Hz}}$ and set-up determined SQL indicates active research in this area.

The physics of the Hamiltonian and splitting

For an NV center gyroscope, the Hamiltonian, a mathematical operator, serves as a representation of various energy states, where the splitting between levels changes based on the interactions between nuclear and electron spins within lattice structure, and the applied magnetic field strength[15]. Equation for Hamiltonian of an NV center is customized for each experimental or modeling setup based on initialization, precession and processing parameters and the NV axes engaged in the process. "Splitting" in the context of NV center gyroscopes Hamiltonian, refers to the creation of new, distinct energy states from an original homogeneous (degenerate) state, driven by interactions with adjacent electromagnetic fields or other spins. Few key splitting mechanisms are discussed below where S is Electron spin vector for the relevant axis, I_N, I_C, the Nitrogen and Carbon spin vectors, Δ is the nominal ZFS value, $\vec{B}$ the external magnetic field, $\gamma_e, \gamma_N, \gamma_C$ the electron, Nitrogen and carbon gyromagnetic ratios, A the hyperfine tensor and Q the ^{14}N quadrupolar term. The NV center Hamiltonian that defines the energy structure involves electronic zero field splitting (ZFS), Zeeman effects, Hyperfine term for coupling between electron spin and ^{14}N nuclear spins and a nuclear quadrupolar component. For gyroscope applications using NV centers, the physical rotation is captured by the Zeeman term enabled by stable triplet state and resulting stable frequency separation[15]. For a single NV center, ^{14}N, in the ground state $S = 1$ electronic triplet state coupled with $I = 1$, the ZFS terms for electron and nuclear spin are ~ 2.87 GHz and -4.945 MHz[6,7]. Additional interactions include coupling with nearby carbon nuclei, microwave drive fields and field misalignments that contribute as noise sources that limit coherence time and sensitivity. The specific terms and interactions included are dependent on the experimental setup parameters such as the isotope choice, magnetic field, axes of application and readout method[6,7].

Electronic Zero Field Splitting (ZFS) $\Delta S_z^2 + E(S_x^2 - S_y^2)$, in NV centers, is caused by the anisotropic dipolar interaction of its two unpaired electron spins[15]. This interaction initiates a triplet state mainly resulting from the longitudinal ZFS component ΔS_z^2. $E(S_x^2 - S_y^2)$, the transverse zero field splitting component, is negligible under normal lattice conditions[18]. This is the characteristic of the NV center defect intrinsically.

Magnetic Dipole-Dipole Interaction, $A_N S * I_N$, occurs in the NV center due to dipole-dipole interactions owing to the presence of a nuclear magnetic moment (non-zero nuclear spin) and an electronic magnetic moment (spin-1). This interaction causes coupling between the electron and nuclear spins, and further splits the triplet electron spin states, originally caused by zero-field splitting (ZFS), into sublevels based on the nuclear spin states prior to introduction of any magnetic field[18].

Electric Quadrupole Interaction (EQI), QI_z^2, refers to the effects of the local electrical field gradient (EFG) on the nuclear quadrupole moment. In NV centers, the ^{14}N nuclei experience this interaction because they have a non-spherical charge distribution, since they are spin-1 systems[18]. In the case of nuclei experiencing EQI, the phenomenon can also be referred to as Nuclear Quadrupole Interaction. Before polarization, the quadrupole interaction separates the $m_I = \pm 1$ and $m_I = 0$ energy levels by -4.945 MHz aligned to the N-V axis with a gyromagnetic ratio $\gamma_N = 0.307$ kHz/G, removing their degeneracy[6,7]. Unlike in certain NMR and atomic gyroscopes, where EQIs can cause unwanted frequency shifts, the EQI in diamond NV center gyroscopes provides a stable frequency separation for measuring rotation-induced shifts[6].

Zeeman shifts, $\gamma_e B * S + \gamma_N B * I_{Nz} + \gamma_C B * I_{Cz}$, are fundamental to NV center gyroscopes. Applying a magnetic field 'B' along the NV (C_3) crystal lattice symmetry axis induces Zeeman shifts in both electron and nuclear ± 1 spin states, coupling the electron spin S, the nitrogen nuclear spin I_N and any nearby carbon nuclear spin I_C within the NV center. Removing degeneracy between the $m_s = \pm 1$ in both electron ground, excited states and separately removes $m_I = \pm 1$ states degeneracy. The creation of triplet states in nuclear and magnetic spin is typically used for measurement, since they are defined, stable, and enable multiple transitions[15].

The NV$^-$ center's optically excited triplet state (^3E) has a room-temperature zero-field splitting of ~ 1.4 GHz between its $m_S = 0$ and $m_S = \pm 1$ sublevels. When an external magnetic field is applied along the NV symmetry axis, the Zeeman effect shifts the $m_S = -1$ sublevel toward $m_S = 0$, at a rate set by the electron gyromagnetic ratio ($\gamma_e \approx 2.8$ MHz/G for NV center).

At an axial field of ~ 500 G the Zeeman energy ($\gamma_e B \approx 1.4$ GHz) matches the excited-state zero-field splitting and the two sublevels become nearly degenerate (i.e., same energy level), this is referred to as the excited-state level anti-crossing (ESLAC). The degeneracy near ESLAC makes direct optical polarization of the ^{14}N nuclear spin efficient. Under green optical pumping the spin-selective intersystem crossing polarizes the NV electron spin into $m_S = 0$. Jaskula et al. noted that near the ESLAC, the hyperfine interaction strongly mixes the nearly degenerate electron–nuclear states thus permitting electron–nuclear flip-flops in the excited state. This results in the transfer of the optically generated electronic polarization to the ^{14}N nucleus. Repeated optical cycles then pump the coupled system into the $|m_S = 0, m_I = +1\rangle$ state with demonstrated polarizations of about 95% at ~ 420 G by this mechanism[19]. The same excited-state flip-flops make the NV fluorescence intensity depend on the nuclear spin state. Jarmola et al. used this principle for their all-optical readout gyroscope. By providing optimal conditions for optical polarization and readout, near ESLAC, both initialization and readout of the sensing nuclei are accomplished optically[6]. Hyperfine term quantifies the strength of internal interaction between the electron and nuclear spin states. The operation of an NV center gyroscope also relies heavily on other physical phenomena especially the optics, waveform interactions such as interference, resonance required to read, isolate and magnify the signaling of the spin states through photoluminescence for optical readout and amplitude frequencies for dispersive readout or the transparency features based EIT readout for resonant cavity-based type gyroscopes[6,7,16].

Results

Over the past 5 years NV center gyroscope research has resulted in ability to improve the sensitivity of these inertial sensors by about 3.5 orders of magnitude to model-predicted $1.5\ \mathrm{m}^{\circ}/\mathrm{s}/\sqrt{\mathrm{Hz}}$[7]. With a diamond Nitrogen vacancy center, using different polarization methods, measurement protocols, error compensation, error mitigation methods or base material used for NV center, these researchers were able to explore parameters that have significant impact on sensitivity on these quantum sensors. The study characteristics, summarized in Table 1 and Table 2, present comparative highlights of the core and explorative papers reviewed. These tables are followed by an applied analysis of the papers.

While the core papers establish feasibility, the exploratory papers focus on niche areas to identify the parameters that can move the sensitivity closer to the SQL (for measurements not involving entanglement) and Heisenberg limit (for measurements utilizing entanglement). The review anticipates future research to increase focus on miniaturization along with further improvements in sensitivity.

Discussion

Theoretical and applied synthesis

Following the first experimental demonstration, improvements in NV center gyroscope sensitivities targeted a combination of bulk polarization, improved optical efficiency and increased coherence times along with some material-based improvements, magnetic shielding and other error compensation mechanisms. Due to the absence of a uniform basis for reporting sensitivity and limited literature, direct quantitative comparison of sensitivity figures is limited. Reported values are a result of experimentally demonstrated vs model predicted, emulated vs physical rotation, optical vs cavity enhanced readout etc. The improvements cited in this review represent a span of experimental and modeled setups, focusing on sensitivity achievable at a scalable form factor, such as MEMS gyroscopes. This is to illustrate the trajectory of theoretical and experimental progress in the field where researchers are exploring various pathways towards achieving the same goal, viz., sensitivity of NMR/SERF gyroscopes with a MEMS scale device.

Polarization

In early 2021, Soshenko et al.[9] demonstrated a proof of concept NV center gyroscope that uses recursive cycling at low magnetic fields for increased polarization and measures nuclear spin indirectly as means to measure angular rotation[9]. That same year, breakthrough experiments were conducted by Jarmola et al.[6] utilizing direct optical polarization enabled by operation near ESLAC (see Background) with a strong external magnetic field at ~ 500 G to maximize polarization, achieve stable nuclear spin states and an all optical direct readout of nuclear spin state[23] with a measured sensitivity of $4.7^\circ/\mathrm{s}/\sqrt{\mathrm{Hz}}$. This pioneering research demonstrated a solid-state NMR gyroscope prototype based on nuclear spins NV centers in diamond. Their implementation included nuclear DQ Ramsey measurement schemes, use of temperature-compensated magnets, magnetic shielding, and robust pulse protocols to reduce the influence of temperature and magnetic field drift for improved stability. Jarmola et al.[6] noted that enhanced fluorescence detection can further improve sensitivity by adjusting the laser power and photon collection efficiency[6]. To help understand the effect of using different engineered NV centers, Soshenko et al.[24] determined that optimization of MW pulse improves population of target state by 15%, but only in the case of dense nitrogen-vacancy ensembles. In addition to polarization, optical efficiency is also being improved. Mounting a diamond onto a conical diamond anvil to improve fluorescence detection demonstrated to improve optical efficiency by a factor of 3.8[25]. Recent experiments using nanodiamond in a nano antenna have demonstrated the optical efficiency approaching unity for $\mathrm{NA} > 0.8$[20] for a single diamond NV center.

Coherence time

Analyzing the nuclear spins of the NV center is generally the superior method for measuring rotation as compared to electron spins for better coherence times, because electron spin coherence dephasing time is $\approx 1.4\ \mu$s while it is $\approx 58\ \mu$s for ^{14}N nuclear spins[26]. Bauch et al.[27] demonstrated more than a $10\times$ increase in NV electron-spin dephasing time (T_2^*) via quantum control, spin bath combined with DQ coherence, showing that improved dephasing time translates to direct improvements in sensitivity. Coherence times can be improved by decoupling methods to minimize the effect of small magnetic field noise that would otherwise shorten spin relaxation and dephasing time. Decoupling methods such as spin bath driving rely on actively refocusing noise fields or averaging out fluctuations. G. Wang et al.[10] demonstrated improved sensitivity in an emulated gyroscope using $^{15}\mathrm{NV}^-$ diamond center, by developing coherence protection based on controlling the NV electronic spin. The strong intrinsic longitudinal field suppresses the transverse magnetic noise, and DQ π pulses then compensate for the effects of hyperfine interactions. This results in the improved coherence time compared to their experiment without coherence protection. They utilized $^{15}\mathrm{NV}^-$ (spin-$1/2$, no quadrupole) in contrast to the core papers that use $^{14}\mathrm{NV}^-$ (spin-1, w/quadrupole), however, they concluded that in spite of no quadrupole noise, the coherence time is not longer for $^{15}\mathrm{NV}^-$, but has the advantage of better control, easier polarization due to fewer available energy states and ability to cancel multiple hyperfine interactions such that coherence time is limited by only longitudinal magnetic field. By identifying and decoupling the underlying microscopic interactions within the diamond material, Han et al.[28] were able to achieve a fourfold improvement to coherence time for electron spin of a single NV center and note its universal applicability for minimizing microscopic noises. Their demonstration exceeded the empirical limit, approaching a physical limit for solid-state

Table 1 Comparative highlights table for core papers.

	Jarmola[6]	Soshenko[9]	H. Wang et al.[7]
Sensor basis	$^{14}NV^-$	$^{14}NV^-$	$^{14}NV^-$
Spin type and Readout Method	Direct optical readout of the nuclear spin	Indirect optical readout of nuclear spin using electron spin	Optical spin state initialization Readout using Resonant cavities
Rotation Type	Rotating platform	Rotating platform	Emulated rotation
Polarization	Direct optical double Radio Frequency (RF)	Recursive Microwave (MW)-RF cycling at low magnetic fields	Nuclear spin-based NV center-cavity coupling under two steady-state two-field driving conditions
Measurement Protocol	DQ Ramsey type pulse seq. for optical readout	DQ Ramsey type pulse seq. for optical readout	Resonator MW signal to achieve EIT for shape, linewidth and amplitude readout
Findings	Demonstrated sensitivity of $4.7°/s/\sqrt{Hz}$.	Proof of concept with a measured sensitivity of $52°/s/\sqrt{Hz}$.	Model-predicted sensitivity of $1.5\ m°/s/\sqrt{Hz}$
Recommendations for improvements	Increasing photon collection efficiency, spin bath driving and better magnetic shielding w/ temp stabilized magnets for improved resilience to environmental magnetic fields.	Further research into low drift compact solid-state gyroscopes.	Applying two field theory to non-linear, bistable and masing without inversion (MWI) regimes in addition to optimizing spin refrigeration and system parameters
Critical assessment	Direct optical readout outperforms the indirect electron mediated readout on sensitivity because of eliminating reliance on the temperature, field sensitive electron spin microwave steps needed for indirect readout. Photon collection losses dominate the gap with SQL.	Indirect readout via electron spin adds microwave steps introducing additional errors requiring the authors to add co-magnetometry, co-thermometer feedback loops that penalized the sensitivity.	This is a predicted model with no experimental gyroscope validation yet. The resonator poses challenges for miniaturization unlike all optical readout designs. Though resonance can magnify errors, for long term use, co-magnetometry was proposed to manage this.

spin coherence time. Pfender et al.[29] focused on avoiding coherence time limitations by mapping the NV state to a nuclear spin, used as a non-volatile memory, can help overcome the spin relaxation time limits.

Processing Improvements

Eisenach et al.[30] demonstrated a cavity enhanced microwave readout method that achieves unity contrast and avoids the photon shot-noise limitations of optical readout by probing spin defects at their resonance frequency using a microwave signal. Kozodaev et al.[16], in their preprint source, proposed dispersive readout using a resonator with two geometrically orthogonal modes to reduce the effect of shot noise on sensitivity by at least a factor of four reporting a magnetic field sensitivity of 0.15 pT. H. Wang et al.[7] adopted a two field interference to directly probe nuclear transitions for cavity enhanced microwave readout. Their model predicted sensitivity is unvalidated with no peer studies yet achieving results at a similar scale.

Magnetic Shielding

The NV center is naturally an excellent magnetometer; hence it is highly sensitive to external fields which can introduce errors in rotation sensing and can reduce the coherence time. So, beyond readout, precise magnetic shielding is required to ensure that the gyroscope measures rotation rather than environmental magnetic noise. Effective shielding systems typically combine materials like low-carbon steel, magnets, and aluminum to shape the magnetic field with extreme accuracy. Shielding made using high-permeability nickel–iron alloy (μ-

Table 2 Comparative highlights table for explorative papers.

	Lubotzky et al.[20]	G. Wang et al.[10]	Isogawa et al.[21]	deQuilettes et al.[22] (Preprint source)
Parameter targeted for improved sensitivity	Photon collection efficiency/ Improvement of optical readout	Coherence time improvements	Use of NV center as a Multifunctional sensor	Temp stable, crystals w/high-quality uniform crystal defects for bulk polarization
Results	Photon collection efficiency $\sim 80\%$ and approaching unity for numerical aperture (NA) $= 0.5$, for NA > 0.8 respectively.	$15\times$ reduction in dephasing time; $\sim 10\times$ improvement in sensitivity for emulated model compared to experimental setup w/o coherence protection.	The authors achieve linear sensitivity scaling for multiple parameters for a more practical quantum sensing future.	Authors achieved 300% improvement in magnetometry using machine learning.
Strategy	Readout efficiency enhanced by integrating them into hybrid metal-dielectric nanoantennas and ultraprecise deterministic positioning.	Hyperfine interactions enhance transverse magnetic noise, but strong longitudinal field suppresses this, using DQ π pulses then compensates for hyperfine interactions for improved coherence time.	Leveraging Bell states measurement and electronic-nuclear spin entanglement, enabled estimation of three parameters from a single measurement sequence, at room temp.	Plasma-enhanced chemical vapor deposition (PE-CVD) can provide the ability to tailor material development for quantum applications.
Recommendations by Original Authors	Next steps were not proposed by the author in this journal research article referenced.	Applications in quantum memories to allow for error correction, and quantum networks with improved coherence time. Using enhanced transverse Zeeman coupling helps understand magnetic noise due to spin bath and will help with magnetic sensing.	Ideal experimental conditions were utilized - repeat under realistic conditions. Future research includes pulse sequence and Hamiltonian techniques development for other parametric measurements such as electric field, temperature, pressure etc.	Tailored materials, and ML framework can optimize other Figure of Merit (FOM)'s for color centers in diamond.
Critical assessment	Focuses on curbing photon collection loss that dominates the $\sim 10^4$ gap to SQL in demonstrated NV gyroscopes but has only been tested on a single NV center while functional gyroscopes require large ensembles on bulk diamond. Transfer of this efficiency gain to rotation sensing is untested.	Strongest quantified coherence gains among reviewed literature. Though the electron-spin only control was tested on a single NV in an emulated configuration, the sensitivity is worse than ensemble demonstrations. The proposed protocol is the primary contribution.	Demonstrates entanglement assisted multiparameter estimation for microwave driven parameters and hence indirectly applicable to gyroscopes. Experimental conditions are ideal per authors, and noise floor is unquantified.	This model-based machine learning guided PE-CVD growth improves the parameters N & T_2^*, on which every other approach depends, the 300% figure-of-merit gain is for magnetometry not rotation sensing. Its benefit to gyroscopes is multiplicative but unvalidated in any rotation demonstration.

metal) redirects or channels external magnetic fields (from the Earth, electronic equipment, or lab noise) through the shield's material instead of penetrating into its interior creating a noise free zone for the sensor. Jarmola et al.[6] used low-carbon steel for this purpose. Though not discussed in most of the papers referenced for this review, externally applied magnetic shielding is the compromise while newer engineered materials and fabrication methods are developed.

Temperature compensated and temperature stable magnets reduce magnetic drifts by minimizing their introduction[6]. In addition to shields, further correction can be applied using co-magnetometry to compensate for bias and errors during post-processing. Passive shielding cannot remove residual magnetic drifts inside the shield; this can however be corrected actively by co-magnetometry. When a stray magnetic field B_z shifts the nuclear precession frequency through the nuclear Zeeman term $\gamma_n B_z$ causing a phase accumulation that is indistinguishable from the rotation signal, it establishes a sensor's noise floor[7]. A co-magnetometer resolves this issue by utilizing a second spin species in the same volume using the NV electron spin to measure the magnetic field concurrently. Because the electron gyromagnetic ratio exceeds the ^{14}N nuclear one by roughly four orders of magnitude, the electron spin is ideal for measuring magnetic field changes while the nuclear spin retains the rotation signal. The electron-spin measurement is then used to compensate the phase accumulation within the noise floor so that rotation can be measured more accurately.

Jaskula et al. demonstrated this principle experimentally in an emulated NV spin gyroscope by having the NV electron-spin ensemble provide active feedback, based on environmental magnetic fields, to stabilize the nuclear Ramsey signal[19]. In the cavity-based proposal of H. Wang et al.[7], a co-magnetometer is implemented as a second microwave probe tone addressing a third nuclear hyperfine sub ensemble. This helped them achieve a magnetic-noise-limited floor of $1\ \mathrm{m}^\circ/\mathrm{s}/\sqrt{\mathrm{Hz}}$ while degrading the EIT rotational sensitivity by less than 1% and provided direct drift correction. Separately, the same platform uses the four crystallographic NV axes for vector rotation resolution while minimizing crosstalk between sub ensembles.

Other factors currently being researched

Error mitigation and advanced materials, fabrication methods also play an important role in improving sensitivity of the NV center gyroscopes. Berzins et al.[31], experimentally characterized the impact of MW phase noise on the noise floor of an NV sensor and proposed ways to predict, suppress these. Isogawa et al.[21], experimentally demonstrate multiparameter estimation using the NV center in diamond, making a case for multifunctional use of NV center multi-sensors. According to the preprint source by D. W. deQuilettes et al.[22], advanced growth techniques, especially plasma-enhanced chemical vapor deposition (PE-CVD) enables development of tailored materials for specific quantum applications.

For the three phases of NV gyroscope sensing described in the background section viz., initialization, precession and processing, there are both intrinsic and external limitations in reaching the SQL for sensitivity of $0.04\ \mathrm{m}^\circ/\mathrm{s}/\sqrt{\mathrm{Hz}}$, for the cavity enhanced EIT readout setup[7]. In the initialization phase, the bulk polarization efficiency can improve the number of data points to minimize some of the errors. For optical readout, a major challenge is photon collection. Due to the high refractive index contrast between diamond and air, a sizable portion of the emitted light is reflected into the diamond instead of escaping to the detector. To reduce this loss, various methods are used, including polishing the diamond for regular emittance, applying anti-reflective coatings, and utilizing condensers or immersion lenses to capture a higher fraction of the fluorescence. Nanodiamonds with nano antennas have been shown to improve photon efficiency to near unity but its applicability to angular momentum sensing needs to be studied. On the other hand, cavity resonance readout-based setups, while more accurate in the short term, lack the stability of full optic readout because they tend to amplify error signals through the inherent resonance mechanism. These are also more difficult to scale down due to the setup requiring a resonator. Isotopic engineering with ^{13}C or ^{15}N nuclei is still under investigation for use in NV centers, denser NV centers also improve polarization in general and are currently being evaluated[24]. Focusing on NV centers based on Nitrogen isotopes vs Silicon vacancy (SiV) centers or rare-earth ion gyroscopes, is a limitation that the author wants to address in the future. Alongside performance enhancements, miniaturization remains a primary goal to move these devices from experimental and prototype setups to practical applications. There are very few groups of researchers focused on NV center gyroscope research, limiting the breadth of selection criteria used. This combined with heterogeneity of readout methods and rotation encoding etc., precludes a quantitative meta-analysis. Currently, there is a strong push for further miniaturization along with sensitivity improvement.

Conclusion

This review paper analyzed various key technological advances and their impact on the sensitivity of an NV center gyroscope. Key challenges include scaling polarization, extending coherence times, and achieving miniaturization[6], which are steadily being overcome. This review concludes that a combination of multiple techniques may be needed to reach the target sensitivity of NV center gyroscopes. These include avoiding coherence limits through mapping the NV state to a nuclear spin memory[29], identifying a more suitable engineered higher NV density isotope, scalable resonant chamber for cavity-based gyroscopes or nanoantenna with nanodiamonds for full optical gyroscopes along with advances in materials, fabrication methods. While this review does not focus on system-level integration challenges such as electronics, magnetic shielding mass, and laser systems, such measures will improve the performance of NV center gyroscopes as noted in the instrumentation errors section.

Diamond NV center gyroscopes are expected to offer distinct advantages for military and defense applications, particularly in environments where GPS is denied or unavailable, potentially for underwater, underground, long duration autonomous missions[2]. Their solid-state nature could make them highly resilient to vibration, temperature fluctuations, pressure changes, and g-shocks, allowing them to possibly outperform MEMS gyroscopes in harsh conditions.

Over a short span, NV center gyroscope research has improved sensitivity of these inertial sensors by about 3.5-order-of-magnitude from an experimentally demonstrated $4.7^\circ/\mathrm{s}/\sqrt{\mathrm{Hz}}$[6] (physical rotation, direct optical readout), to model-predicted $1.5\ \mathrm{m}^\circ/\mathrm{s}/\sqrt{\mathrm{Hz}}$[7] (emulated rotation, cavity-enhanced readout). The SQL for NV center ensemble sensor modeled by H. Wang evaluates to $0.04\ \mathrm{m}^\circ/\mathrm{s}/\sqrt{\mathrm{Hz}}$ versus the $0.1\ \mathrm{m}^\circ/\mathrm{s}/\sqrt{\mathrm{Hz}}$ benchmark for the smaller ensembles from previous NV center gyroscope setups[7]. Although literature reviewed is limited and it is not feasible to have a direct performance comparison across studies that use different readout methods, rotation encoding approaches, and experimental scales; based on the critical analysis of the literature in the field the author finds that the NV center gyroscopes' performance is rapidly improving and with continued research, these sensors can attain the goals of sensitivity approaching gas phase NMR and miniaturization approaching MEMS scale. Such improvements combined with the potential of a solid-state, mass producible components can help NV center gyroscopes approach the cost profile of MEMS in lieu of navigation-class gyroscopes, making these quantum sensing devices well positioned for wide adoption in the defense and civilian applications[9].

Acknowledgements

I sincerely thank Dr. Damián Pitalúa-García and the course teaching assistant Ms. Ruhi Shah from Cambridge Center for International Research summer scholar program for introducing me to Quantum physics and encouraging me to perform independent research and Ms. Shah's continued support over the past year as my mentor. I would also like to thank my friends and family for their encouragement.

References

1 N. El-Sheimy and A. Youssef, Inertial sensors technologies for navigation applications: state of the art and future trends. Satellite Navigation. Vol. 1, pg. 2, 2020. https://doi.org/10.1186/s43020-019-0001-5.

2 H. Pei, W. Fan, L. Duan, F. Liu, H. Pang, R. Li, Y. Feng, Y. Liu, Y. Wang, H. Yuan, J. Tang, H. Zheng, J. Qin and W. Quan, Navigation in the future: review of quantum sensing in navigation. Science China Physics, Mechanics & Astronomy. Vol. 68, pg. 290301, 2025. https://doi.org/10.1007/s11433-025-2699-1.

3 Y. Chang, S.-A. Wan and J. Qin, Quadrupole effects on nuclear-magnetic-resonance gyroscopes. Physical Review A. Vol. 102, pg. 013507, 2020. https://doi.org/10.1103/PhysRevA.102.013507.

4 T. Walker and M. Larsen, Spin-exchange pumped nmr gyros. Advances In Atomic, Molecular, and Optical Physics. Vol. 65, pg. 373–401, 2016. https://doi.org/10.1016/bs.aamop.2016.04.002.

5 T. W. Kornack, R. K. Ghosh and M. V. Romalis, Nuclear spin gyroscope based on an atomic comagnetometer. Physical Review Letters. Vol. 95, pg. 230801, 2005. https://doi.org/10.1103/PhysRevLett.95.230801.

6 A. Jarmola, S. Lourette, V. M. Acosta, A. G. Birdwell, P. Blümler, D. Budker, T. Ivanov and V. S. Malinovsky, Demonstration of diamond nuclear spin gyroscope. Science Advances. Vol. 7, pg. eabl3840, 2021. https://doi.org/10.1126/sciadv.abl3840.

7 H. Wang, S. Wu, K. Jacobs, Y. Duan, D. R. Englund and M. E. Trusheim, Cavity-enhanced solid-state nuclear spin gyroscope. Physical Review Letters. Vol. 134, pg. 183603, 2025. https://doi.org/10.1103/PhysRevLett.134.183603.

8 *V. Passaro and A. Cuccovillo and L. Vaiani and M. De Carlo and C. E. Campanella* Gyroscope technology and applications: a review in the industrial perspective. Sensors. Vol. 17, pg. 2284, 2017. https://doi.org/10.3390/s17102284.

9 V. V. Soshenko, S. V. Bolshedvorskii, O. Rubinas, V. N. Sorokin, A. N. Smolyaninov, V. V. Vorobyov and A. V. Akimov, Nuclear spin gyroscope based on the nitrogen vacancy center in diamond. Physical Review Letters. Vol. 126, pg. 197702, 2021. https://doi.org/10.1103/PhysRevLett.126.197702.

10 G. Wang, M.-T. Nguyen, D. W. deQuilettes, E. Price, Z. Hu, D. A. Braje and P. Cappellaro, Emulated nuclear spin gyroscope with ^{15}NV centers in diamond. Physical Review Applied. Vol. 22, pg. 044016, 2024. https://doi.org/10.1103/PhysRevApplied.22.044016.

11 O. J. Woodman, An introduction to inertial navigation. University of Cambridge Computer Laboratory, Technical Report UCAM-CL-TR-696. 2007. https://www.cl.cam.ac.uk/techreports/UCAM-CL-TR-696.pdf.

12 D. A. Hopper, H. J. Shulevitz and L. C. Bassett, Spin readout techniques of the nitrogen-vacancy center in diamond. Micromachines. Vol. 9, pg. 437, 2018. https://doi.org/10.3390/mi9090437.

13 M. P. Ledbetter, K. Jensen, R. Fischer, A. Jarmola and D. Budker, Gyroscopes based on nitrogen-vacancy centers in diamond. Physical Review A. Vol. 86, pg. 052116, 2012. https://doi.org/10.1103/PhysRevA.86.052116.

14 A. A. Wood, E. Lilette, Y. Y. Fein, N. Tomek, L. P. McGuinness, L. C. L. Hollenberg, R. E. Scholten and A. M. Martin, Quantum measurement of a rapidly rotating spin qubit in diamond. Science Advances. Vol. 4, pg. eaar7691, 2018. https://doi.org/10.1126/sciadv.aar7691.

15 M. W. Doherty, N. B. Manson, P. Delaney, F. Jelezko, J. Wrachtrup and L. C. L. Hollenberg, The nitrogen-vacancy colour centre in diamond. Physics Reports. Vol. 528, pg. 1–45, 2013. https://doi.org/10.1016/j.physrep.2013.02.001.

16 A. M. Kozodaev, I. S. Cojocaru, S. M. Drofa, P. G. Vilyuzhanina, A. Chernyavskiy, V. G. Vins, A. N. Smolyaninov, S. Y. Kilin, S. V. Bolshedvorskii, V. V. Soshenko and A. V. Akimov, Dispersive readout

with two orthogonal modes of a dielectric cavity. Preprint at http://arxiv.org/abs/2512.07356. 2025. https://doi.org/10.48550/arXiv.2512.07356.

17 T. Xie, Z. Zhao, X. Kong, W. Ma, M. Wang, X. Ye, P. Yu, Z. Yang, S. Xu, P. Wang, Y. Wang, F. Shi and J. Du, Beating the standard quantum limit under ambient conditions with solid-state spins. Science Advances. Vol. 7, pg. eabg9204, 2021. https://doi.org/10.1126/sciadv.abg9204.

18 S. Felton, A. M. Edmonds, M. E. Newton, P. M. Martineau, D. Fisher, D. J. Twitchen and J. M. Baker, Hyperfine interaction in the ground state of the negatively charged nitrogen vacancy center in diamond. Physical Review B. Vol. 79, pg. 075203, 2009. https://doi.org/10.1103/PhysRevB.79.075203.

19 J.-C. Jaskula, K. Saha, A. Ajoy, D. J. Twitchen, M. Markham and P. Cappellaro, Cross-sensor feedback stabilization of an emulated quantum spin gyroscope. Physical Review Applied. Vol. 11, pg. 054010, 2019. https://doi.org/10.1103/PhysRevApplied.11.054010.

20 B. Lubotzky, H. Abudayyeh, N. Nikolay, O. Benson and R. Rapaport, Approaching unity photon collection from nv centers via ultra-precise positioning of nanodiamonds in hybrid nanoantennas. APL Quantum. Vol. 2, pg. 036106, 2025. https://doi.org/10.1063/5.0272913.

21 T. Isogawa, G. Wang, B. Li, Z. Hu, S. Nishimura, A. Kanamoto, H. Yuan and P. Cappellaro, Entanglement-assisted multiparameter estimation with a solid-state quantum sensor. PRX Quantum. Vol. 7, pg. 020307, 2026. https://doi.org/10.1103/kqfr-bbfx.

22 D. W. deQuilettes, E. Price, L. M. Pham, A. Kurlej, S. Vattam, A. Melville, T. Osadchy, B. Li, G. Wang, C. N. Muniz, P. Cappellaro, J. M. Schloss, J. L. Mallek and D. A. Braje, Machine learning enables optimization of diamond for quantum applications. Preprint at http://arxiv.org/abs/2510.22121. 2025. https://doi.org/10.48550/arXiv.2510.22121.

23 A. Jarmola, I. Fescenko, V. M. Acosta, M. W. Doherty, F. K. Fatemi, T. Ivanov, D. Budker and V. S. Malinovsky, Robust optical readout and characterization of nuclear spin transitions in nitrogen-vacancy ensembles in diamond. Physical Review Research. Vol. 2, pg. 023094, 2020. https://doi.org/10.1103/PhysRevResearch.2.023094.

24 V. V. Soshenko, I. S. Cojocaru, S. V. Bolshedvorskii, O. R. Rubinas, V. N. Sorokin, A. N. Smolyaninov and A. V. Akimov, Optimal microwave control pulse for nuclear spin polarization and readout in dense nitrogen-vacancy ensembles in diamond. Physica Status Solidi (b). Vol. 260, pg. 2200613, 2023. https://doi.org/10.1002/pssb.202200613.

25 M. Omar, A. Conta, A. Westerhoff, R. Hasse, G. Chatzidrosos, D. Budker and A. Wickenbrock, Diamond-optic enhanced photon collection efficiency for sensing with nitrogen-vacancy centers. Optics Letters. Vol. 48, pg. 2512, 2023. https://doi.org/10.1364/OL.486998.

26 G. Fuchs, G. Burkard, P. Klimov and D. Awschalom, A quantum memory intrinsic to single nitrogen-vacancy centres in diamond. Nature Physics. Vol. 7, pg. 789–793, 2011. https://doi.org/10.1038/nphys2026.

27 E. Bauch, C. A. Hart, J. M. Schloss, M. J. Turner, J. F. Barry, P. Kehayias, S. Singh and R. L. Walsworth, Ultralong dephasing times in solid-state spin ensembles via quantum control. Physical Review X. Vol. 8, pg. 031025, 2018. https://doi.org/10.1103/PhysRevX.8.031025.

28 S. Han, X. Ye, X. Zhou, Z. Liu, Y. Guo, M. Wang, W. Ji, Y. Wang and J. Du, Solid-state spin coherence time approaching the physical limit. Science Advances. Vol. 11, pg. eadr9298, 2025. https://doi.org/10.1126/sciadv.adr9298.

29 M. Pfender, N. Aslam, H. Sumiya, S. Onoda, P. Neumann, J. Isoya, C. A. Meriles and J. Wrachtrup, Nonvolatile nuclear spin memory enables sensor-unlimited nanoscale spectroscopy of small spin clusters. Nature Communications. Vol. 8, pg. 834, 2017. https://doi.org/10.1038/s41467-017-00964-z.

30 E. R. Eisenach, J. F. Barry, M. F. O'Keeffe, J. M. Schloss, M. H. Steinecker, D. R. Englund and D. A. Braje, Cavity-enhanced microwave readout of a solid-state spin sensor. Nature Communications. Vol. 12, pg. 1357, 2021. https://doi.org/10.1038/s41467-021-21256-7.

31 A. Berzins, M. S. Ziabari, Y. Silani, I. Fescenko, J. T. Damron, J. F. Barry, A. Jarmola, P. Kehayias, B. A. Richards, J. Smits and V. M. Acosta, The impact of microwave phase noise on diamond quantum sensing. Physical Review Research. Vol. 6, pg. 043148, 2024. https://doi.org/10.1103/PhysRevResearch.6.043148.